The Hippo pathway mediates resistance to cytotoxic drugs

Taranjit S. Gujral[1,2], and Marc W. Kirschner[1*]

[1]Department of Systems Biology, Harvard Medical School, Boston, MA

[2]Current address: Division of Human Biology, Fred Hutchinson Cancer Research Center, Seattle, WA.

* Corresponding author. E-mail: marc@hms.harvard.edu

Running title: Hippo pathway mediates drug sensitivity

Keywords: Hippo pathway/YAP/drug resistance/ transporters/gemcitabine

This supplementary file includes:

Supplementary Figures S1, S2, S3, S4, S5, S6, S7, S8

Supplementary Tables S1, S2, S3, S4

Extended Experimental Procedures

Antibodies

Primary antibodies were obtained from the following sources: rabbit phosphor-YAP (S127) (Cell Signaling Technology, Beverly, MA; cat. # 13008), rabbit anti-YAP (Cell Signaling Technology, Beverly, MA; cat. # 14074), mouse anti-β-actin (Sigma-Aldrich, Inc., St. Louis, MO; cat. #A1978).

Reverse-Phase Protein Microarray

Cell lysates prepared from various pancreatic cancer cell lines were printed using Aushon 2470 Arrayer (Aushon Biosystems). Validation of antibodies, staining, and analysis of array data was performed as described previously (1).

3D spheroid assay

Cancer cell lines were seeded at a 5x10 cells per well in 96-well ultra-low adherence plates (Costar) and briefly spun down at 1000rpm for 5 minutes. After 2 days, cells were treated with small molecule inhibitors at varying concentrations. Growth of spheroids was monitored using live cell imaging every 2-3 hours for 4-7 days in the Incucyte ZOOM system (Essen) or as end point assay using CellTiter-Glo luminescent cell viability assay (Promega).

Generation of YAPS6A overexpression cell lines

Cell lines (Panc02.13, Panc10.05 or Miapaca2) were transfected with YAPS6A constructs (Addgene plasmid #42562) using Lipofectamine (Invitrogen, Carlsbad, CA) following the manufacturer's instructions and 48 hour post-transfection selected in 5-10 μg/ml Blasticidin (InvivoGen, San Diego, CA). The clones screened for YAPS6A expression by Western blot. Stable cell lines were maintained in complete medium and 5 μg/ml Blasticidin.

RNA extraction and quantitative real-time PCR

Cells were serum-starved for 24 h and total cellular RNA was isolated using an RNeasy Mini Kit (QIAGEN, Santa Clara, CA). mRNA levels for the EMT-related genes were determined using the RT^2 profiler™ qPCR array (SA Biosciences Corporation, Frederick, MD). Briefly, 1 μg of total RNA was reverse transcribed into first strand cDNA using an RT^2 First Strand Kit (SA Biosciences). The resulting cDNA was subjected to qPCR using human gene-specific primers for 75 different genes, and five housekeeping genes (B2M, HPRT1, RPL13A, GAPDH, and ACTB). The qPCR reaction was performed with an initial denaturation step of 10 min at 95°C, followed by 15 s at 95°C and 60 s at 60°C for 40 cycles using an Mx3000P™ QPCR system (Stratagene, La Jolla, CA).

The mRNA levels of each gene were normalized relative to the mean levels of the five housekeeping genes and compared with the data obtained from unstimulated, serum-starved cells using the $2-\Delta\Delta Ct$ method. According to this method, the normalized level of a mRNA, X, is determined using equation 1: (1)

$$X = 2^{-Ct(\mathrm{GOI})}/2^{-Ct(\mathrm{CTL})} \quad (1)$$

where Ct is the threshold cycle (the number of the cycle at which an increase in reporter fluorescence above a baseline signal is detected), GOI refers to the gene of interest, and CTL refers to a control housekeeping gene. This method assumes that Ct is inversely proportional to the initial concentration of mRNA and that the amount of product doubles with every cycle.

Protein isolation and quantitative western blotting

Cells were rinsed in Phosphate Buffered Saline (PBS) and lysed in Lysis Buffer (20 mM Tris-HCl, 150 mM NaCl, 1% Triton X-100 (v/v), 2 mM EDTA, pH 7.8 supplemented with 1 mM sodium orthovanadate, 1 mM phenylmethylsulfonyl fluoride (PMSF), 10 µg/mL aprotinin, and 10 µg/mL leupeptin). Protein concentrations were determined using the BCA protein assay (Pierce, Rockford, IL) and immunoblotting experiments were performed using standard procedures. For quantitative immunoblots, primary antibodies were detected with IRDye 680-labeled goat-anti-rabbit IgG or IRDye 800-labeled goat-anti-mouse IgG (LI-COR Biosciences, Lincoln, NE) at 1:5000 dilution. Bands were visualized and quantified using an Odyssey Infrared Imaging System (LI-COR Biosciences).

Kaplan-Meier Survival Analysis

Kaplan Meier survival curves of pancreatic cancer patients were generated using PROGgene using combined signature graph function and Kaplan Meier plotter web-based tools (2-4).

Confocal imaging

Panc02.13 cells were cultured on Lab-Tek II chamber glass slides (Nalge Nunc, Naperville, IL) or on 24-well glass bottom dishes (MatTek Corporation). Cells were fixed in 4% paraformaldehyde for 15 min at room temperature, washed in PBS, permeabilized with 0.1% Triton X-100, and blocked for 60 min with PBS containing 3% BSA (w/v). Cells were immunostained with the appropriate antibody, following by immunostaining with Alexa Fluor 488-labeled goat-anti-rabbit antibody (Molecular Probes, Eugene, OR). Nuclei were counterstained with Hoescht 33342 (Sigma-Aldrich, St. Louis, MO). Fluorescent micrographs were obtained using a Nikon A1R point scanning confocal microscope. Individual channels were overlaid using ImageJ software (National Institutes of Health, Bethesda, MD).

Measuring gemcitabine efflux

Panc02.13. cells expressing GFP or YAPS6A plasmid were treated with radiolabeled gemcitabine (0.5µM) for one hour. Cells were washed twice with PBS and incubated in fresh medium. Medium was collected over the time course of 24 hours and radioactivity was measured using scintillation counter.

Profiling drug transporters

mRNA expression of drug transporters was profiled using Human Drug transporters PCR Array from SA Biosciences (cat # PAHS-070Z) using manufacturer's instructions.

Tumorigenicity in Nude Mice

All *in vivo* experiments were performed using 6-week-old to 8-week-old athymic nude mice. Mice were maintained in laminar flow rooms with constant temperature and humidity. Miapaca2 or Panc02.13 cells were inoculated subcutaneously (s.c.) into each flank of the mice. Cells (2×10^6 in suspension) were injected on day 0, and tumor growth was followed every 2 to 3 days by tumor diameter measurements using vernier calipers. Tumor volumes (V) were calculated using the formula: $V = AB^2/2$ (A, axial diameter; B, rotational diameter). When the outgrowths were ~200 mm3, mice were divided at random into two groups (control and treated, n=3-8). The treated group received gemcitabine injection or saline control on alternate days (MWF) for 2 weeks.

Patient-derived xenograft (PDX) models

PDX models were established by Champions Oncology (Baltimore, MD) as described previously (5). Drug response to 20 PDX models was obtained from Champions TumorGraft® Database (http://database.championsoncology.com/).

Immunohistochemistry

Human primary tumor tissue slides were obtained from Champions Oncology (Baltimore, MD). Immunohistochemistry using anti YAP1 antibody (Abcam Cat # ab52771) was performed as previously described (6). For negative controls, primary antibody was omitted. The intensity of YAP staining was assessed by an independent pathologist (Dr. Langxing Pan) using a four-grade scale: “0” is negative. “0.5“ is borderline staining with no significance. “1” is weak staining. “1.5” is weak staining with foci of moderate staining. “2“ is moderate staining. “2.5“ is moderate staining with foci of strong staining. “3“ is homogeneous strong staining. “3.5“ is very strong and homogeneous staining with no significant background. “4” is over staining usually with background staining. YAP scoring index was calculated based on staining intensity * % of positive target cells.

Intra-tumor gemcitabine measurements

LC–MS/MS was used to simultaneous quantification of gemcitabine, and it’s inactive metabolite dFdU in tumour tissue from a mouse xenograft model of pancreatic cancer as described previously (7).

Supplementary Figures and Legends

Fig. S1. Dose response curves of gemcitabine treated pancreatic cancer A, liver cancer and untransformed (B) cell lines. The respective EC_{50} for each cell line is also indicated. Growth factor stimulation of pancreatic cancer cells does not affect gemcitabine response**. C.** Bar graphs showing changes in cell viability at 72hr (top) and 96hr (bottom) post stimulation with a combination of growth factor and gemcitabine. Cells were also treated with PBS control and gemcitabine alone. **D**. Growth factor stimulation activated their cognate downstream signaling proteins. Bar graphs showing activities of six downstream signaling proteins following stimulation with 15 growth factors.

Fig. S2. Changes in extrinsic factors do not affect gemcitabine response. A. Plot showing magnesium concentration increases cell growth in Bxpc3 cells in a dose-dependent manner. **B.** High magnesium concentration (5μM) has no effect on gemcitabine response in high crowding conditions. Bxpc3, Aspc1 and Panc10.05 cells grown in high crowding conditions were exposed to gemcitabine and cell viability was measured using live cell imaging. **C**. Conditioned media from Panc1 or human dermal fibroblast (HDF) cells has no effect on gemcitabine response in high crowding conditions. **D**. Co-culturing of sparse GFP-labeled Pan02.13 cells achieved high overall cell density produced the same resistance to gemcitabine found in dense tumor cell culture. Cells grown in high crowding conditions do not acquire intrinsic resistance to apoptosis. **E.** A plot showing levels of 29 apoptosis-related signaling proteins in Panc02 cells grown in low crowding (LD) or high crowding conditions (HD). Levels of apoptotic proteins were measured using antibody arrays as described in materials and methods. **F.** Ultra-violet (UV)-induced apoptosis is not affected by cell crowding conditions. Panc02.13 cells grown in varying crowding conditions were exposed to medium strength UV for 10 sec. Cells were then lysed and whole cell lysates were subjected to western blotting. Western blots showing activities of cleaved caspase3, 7 and PARP.

Fig. S3. Cell crowding-dependent response to cytotoxic drugs in pancreatic cancer. **A**. Plots showing the effect of six cytotoxic drugs on growth of seven pancreatic cancer cell lines under sparse and dense conditions. The efficacy of gemcitabine, doxorubicin was crowding-dependent while the effects of camptothecin paclitaxel, docetaxel and oxaliplatin were largely crowding-independent. Hippo-YAP pathway is activated in pancreatic cancer cells at high crowding conditions. **B.** Plot showing changes in phosphorylation of S6 ribosomal protein with cell crowding in six different pancreatic cancer cell lines. **C.** A heatmap showing changes in phosphorylation of growth factor signaling proteins such as Akt, Erk, Mek, Src, and S6 in Aspc1 cells. **D.** Western blots showing cell crowding-dependent changes in YAP phosphorylation (S127) in four pancreatic cancer cell lines. Knockdown of YAP decreases pancreatic cell proliferation. **E.** Western blots showing knockdown of YAP using two different shRNA in three pancreatic cell lines. Blots were also probed with β-actin for loading control. **F**. Plots showing growth of three pancreatic cancer cell lines expressing control or shRNA targeting YAP.

Fig. S4. Cell crowding-dependent affect of verteporfin on pancreatic cancer cell growth. A. Verteporfin treatment potently slows down growth of Panc02.13 cells when grown in low crowding conditions. **B.** Dose response curves of Panc02.13 cells treated with verteporfin, gemcitabine or combination of verteporfin and gemcitabine (50nM) in a 3D-spheroid assay. EC_{50} of verteporfin in 3D-spheroid and low crowding condition is also indicated. **C.** Inactivation of Hippo pathway restores sensitivity to verteporfin in 3D-spheroid assay. Dose response curve of Panc02 cells expressing control-shRNA or shRNA targeting *NF2*. EC_{50} for each condition is also indicated. Hippo pathway inactivation mildly increases cell growth of pancreatic cancer cells. **D.** Western blots showing expression of V5-YAPS6A in Panc10.05 and Panc02.13 cells. **E.** Western blots showing expression of YAPS6A and NF2 knockdown increases phosphorylation of S6 ribosomal protein. Blots were also probed with β-actin for loading control. **F.** Plot showing mRNA expression of YAP-TEAD target genes in Panc02 cells expressing GFP or YAPS6A in high crowding conditions. **G.** YAPS6A expression or NF2 depletion mildly increases cell growth in Panc02 cells. **H.** YAPS6A expression in Panc10.05 cells increases number of EdU-positive cell population in high crowding conditions.

Fig. S5. Hippo pathway inactivation sensitizes cells to gemcitabine and 5-FU. A. Hippo inactivation (YAPS6A) expression sensitizes Panc02 cells to 5-FU in high crowding conditions. **B.** YAPS6A expression increases apoptosis in gemcitabine treated Panc02 cells. Panc02 cells expressing YAPS6A or vector control were treated with varying doses of gemcitabine. Apoptosis was scored using nucview caspase 3/7 reagent. Plots show number of GFP positive (cleaved caspase3/7) cells upon gemcitabine treatment. **C.** Plot showing change in cell viability in gemcitabine treated Panc2 expressing vector or YAPS6A cells. **D.** YAPS6A expression sensitizes cells to gemcitabine in a soft agar colony formation assay. **E.** Hippo pathway inactivation increases action of several FDA-approved oncology drugs. Dose response curves of Panc02 cells expressing GFP or YAPS6A treated with 15 FDA-approved oncology drugs. **F**. Stability of gemcitabine in conditioned media over 5-day period. Plots showing gemcitabine and dFdU **(G)** from media-alone or from Panc02.13 cells collected over five days. Relative concentration of gemcitabine and dFdU was measured using LC/MS. **H.** Representative Multiple-Reaction Monitoring (MRM) Chromatograms of gemcitabine and dFdU from Pan02 or media only at day 1.

Fig. S6. Hippo pathway inactivation decreases drug transport pumps. A. Bar graph showing relative mRNA expression of ABCB4, ABCC3 and MVP in Panc02.13 cells expressing control-shRNA or NF2-shRNA. **B.** YAPS6A expression decreases expression of several transporters while the expression gemcitabine uptake pump (SLC29A1) remains unaffected. **C.** Protein levels of LRP and ABCG2 in Panc02.13 cells expressing YAPS6A, or vector control or NF2-shRNA. **D.** Western blots showing cell crowding-dependent changes in protein levels of ABCG2 and LRP. **E.** Hippo inactivation decreases levels of cytidine deaminase (CDA). YAPS6A expression in Panc1 cells decreases mRNA expression of CDA. mRNA expression of dCK remains unaffected. **F.** NF2 depletion in Patu8988S and YAPC cells decreases CDA levels. **G.** Western

blot showing expression of YAPS6A in Patu8902 cells decreases CDA protein levels. **H.** Verteporfin treatment increases mRNA expression of CDA in Panc02.13 cells. **I.** Gemcitabine resistant-MKN28 showed high levels of CDA. **J.** Western blots showing restoring LATS2 expresion in H2052 mesothelioma cells increases CDA protein levels. The levels of dCK remain unchanged. **K.** LKB1 knockout cells showed decreased CDA levels. **L, M.** Plots showing normalized protein levels of phospho-YAP and CDA in A549 (*STK11* mut) and Calu-1 (*STK11*-WT) cells under various crowding conditions.

Fig. S7. YAP activation sensitizes pancreatic tumors to gemcitabine in mouse xenograft models. A. Gemcitabine treatment of YAPS6A expressing Panc02.13 xenografts showed significantly reduced tumor growth in nude mice. Parental (left) or YAPS6A expressing Panc02.13 cells (right) were subcutaneously injected into athymic mice. When the outgrowths were approximately 200 mm^3, mice were divided at random into two groups (vehicle control, gemcitabine). **B.** Bar graph showing relative levels of cleaved caspase 7 and phosphor-H2aX in Miapaca2 xenografts. **C.** Poor correlation between gemcitabine response and tumor doubling time in PDX models (r=-0.07). **D.** Plots showing tumor growth inhibition in response to other cytotoxic drugs is not affected by YAP levels ($p>0.05$). **E.** High levels of Hippo-YAP downstream gene target is associated with prolonged patient survival in pancreatic cancers in two independent studies. Kaplan-Meier curves of overall survival of pancreatic cancer patients with low or high levels of YAP- TEAD downstream targets.

Fig. S8. Hippo pathway inactivation correlates with better overall survival in pancreatic, lung and gastric cancers. A. Kaplan–Meier plot of lung cancer patients with low or high levels of CTGF. **B.** Kaplan–Meier plot of gastric cancer patients treated with 5-FU-based chemotherapy with Hippo activation (levels of NF2, left) or hippo inactivation (levels of CTGF, right). **C**. Kaplan–Meier plots sowing overall survival of pancreatic cancer patients with low or high levels of Hippo-YAP independent transporter gene signature. **D.** Drug modulating pumps and CDA levels are upregulated in pancreatic cancers. Plots showing increased relative expresion levels of ABCC3, MVP and **(E)** CDA in pancreatic tumor samples compared with normal tissue. **F.** Levels of YAP-TEAD target genes are not altered in pancreatic tumor samples.

Table S1. Inconsistency in gemcitabine response has been observed in literature for these cell lines. Literature curated gemcitabine IC50 in nanomolar.

Cell line	(8)	(9)	(10)	(11)	(12)	(13)	(14)	(15)	(16)	(17)
Aspc1	8269			310		14.59			30.5	3500
BxPc3	0.5		18	5910	50			10000		22300
Capan2	91200		12					2000		
CFPAC1		33								
DANG										
MiapCa2	0.18	298	40	11430	160	35.87	9700			22700
Panc02.13										
Panc08.13	2150									
Panc1		1161	50	58240	480		141000		52.3	27000
Panc10.05	0.07									
Patu8902										
Patu8988-S										
PSN-1										
SW1990	6.6									
YAPC	22100000									

Table S2. Pancreatic cancer cell lines with genetic and clinical characteristics used in the current study.

Cell line	Source	Cell type	Age	Gender	KRAS	p53	p16	Disease	Differentiation
Aspc1	Ascites	Ductal	62	Female	G12D	C135F	WT	Adenocarcinoma	Moderate-Well
BxPc3	Primary tumor	Ductal	16	Female	WT	Y220C	WT/Meth	Adenocarcinoma	Moderate
Capan2	Liver met	Ductal	56	Male	G12V	WT	WT	Adenocarcinoma	Well
CFPAC1	Liver met	Ductal	26	Male	G12V	C242R	WT/Meth	Adenocarcinoma	Well
DANG	Primary tumor	Ductal							Well
MiapCa2	Primary tumor	Ductal	65	Male	G12C	R248W	HD	Carcinoma	Poor-Moderate
Panc02.13	Primary tumor								
Panc08.13	Primary tumor								
Panc1	Primary tumor	Ductal	56	Male	G12D	R273H	HD	Epithelioid carcinoma	Poor

Panc10.05	Primary tumor			Male	G12D	I255N		Adenocarcinoma	
Patu8902	Primary tumor					C176S			
Patu8988-S	Liver met					P151S			
PNS-1	Primary tumor				G12R	K132Q	HD	Adenocarcinoma	
SW1990	Spleen				G12D	WT	HD		Moderate-Well
YAPC	Ascites	Ductal	43	Male		H179R			

References

1. Luckert K*, et al.* (2012) A dual array-based approach to assess the abundance and posttranslational modification state of signaling proteins. *Sci Signal* 5(206):pl1.
2. Goswami CP & Nakshatri H (2013) PROGgene: gene expression based survival analysis web application for multiple cancers. *Journal of clinical bioinformatics* 3(1):22.
3. Gao J*, et al.* (2013) Integrative analysis of complex cancer genomics and clinical profiles using the cBioPortal. *Science signaling* 6(269):pl1.
4. Győrffy B, Surowiak P, Budczies J, & Lánczky A (2013) Online survival analysis software to assess the prognostic value of biomarkers using transcriptomic data in non-small-cell lung cancer. *PloS one* 8(12):e82241.
5. Khor TO*, et al.* (2015) A patient-centric repository of PDX models for translational oncology research. *Cancer research* 75(15 Supplement):3219-3219.
6. Shi S-R*, et al.* (1999) Sensitivity and detection efficiency of a novel two-step detection system (PowerVision) for immunohistochemistry. *Applied Immunohistochemistry & Molecular Morphology* 7(3):201.
7. Bapiro TE*, et al.* (2011) A novel method for quantification of gemcitabine and its metabolites 2', 2'-difluorodeoxyuridine and gemcitabine triphosphate in tumour tissue by LC–MS/MS: comparison with 19F NMR spectroscopy. *Cancer chemotherapy and pharmacology* 68(5):1243-1253.
8. Yang W*, et al.* (2013) Genomics of Drug Sensitivity in Cancer (GDSC): a resource for therapeutic biomarker discovery in cancer cells. *Nucleic acids research* 41(D1):D955-D961.

9. Hong SP, Wen J, Bang S, Park S, & Song SY (2009) CD44-positive cells are responsible for gemcitabine resistance in pancreatic cancer cells. *International journal of cancer* 125(10):2323-2331.
10. Duxbury MS, Ito H, Zinner MJ, Ashley SW, & Whang EE (2004) Inhibition of SRC tyrosine kinase impairs inherent and acquired gemcitabine resistance in human pancreatic adenocarcinoma cells. *Clinical cancer research* 10(7):2307-2318.
11. Huanwen W*, et al.* (2009) Intrinsic chemoresistance to gemcitabine is associated with constitutive and laminin-induced phosphorylation of FAK in pancreatic cancer cell lines. *Mol Cancer* 8(125):21.
12. Parsels LA*, et al.* (2009) Gemcitabine sensitization by checkpoint kinase 1 inhibition correlates with inhibition of a Rad51 DNA damage response in pancreatic cancer cells. *Molecular cancer therapeutics* 8(1):45-54.
13. Shi X*, et al.* (2002) Acquired resistance of pancreatic cancer cells towards 5-Fluorouracil and gemcitabine is associated with altered expression of apoptosis-regulating genes. *Oncology* 62(4):354-362.
14. Giovannetti E, Mey V, Danesi R, Mosca I, & Del Tacca M (2004) Synergistic cytotoxicity and pharmacogenetics of gemcitabine and pemetrexed combination in pancreatic cancer cell lines. *Clinical cancer research* 10(9):2936-2943.
15. Humbert M*, et al.* (2010) Masitinib combined with standard gemcitabine chemotherapy: in vitro and in vivo studies in human pancreatic tumour cell lines and ectopic mouse model. *PLoS One* 5(3):e9430.
16. Modrak DE, Leon E, Goldenberg DM, & Gold DV (2009) Ceramide regulates gemcitabine-induced senescence and apoptosis in human pancreatic cancer cell lines. *Molecular Cancer Research* 7(6):890-896.
17. Mori-Iwamoto S*, et al.* (2008) A proteomic profiling of gemcitabine resistance in pancreatic cancer cell lines. *Mol Med Rep* 1:429-434.

Table S3. Presence of mutations/deletions in Hippo pathway genes in clinical studies of different cancer types.

Indication	NF2	STK11	LATS2	LATS1
Melanoma	0	0	0	0
Stomach	0	0	5	5
Colon	0	0	0	0
Lung	0	18	5.8	0
Colon	0	0	0	0
Uterine	0	0	5.4	0
Esophageal	0	0	0	0
Bladder	0	0	0	0
Prostate	0	0	8.2	0
Head & Neck	0	0	0	0
Mesothelioma	30	0	0	0
Kidney	7.5	0	0	0
Pancreatic	5.6	0	0	0
Ovarian	0	4.8	0	0
Adenoid cyctic c	0	0	0	15
Lymphoid neopl	0	0	0	8

Table S4. Characteristics of PDX models obtained from Champions TumorGraft® Database (http://database.championsoncology.com/)

Model	Cancer type	Histology	Tumor statu	Harvest site	Disease	Age	Gender	ubling t	Drug	%TGI	YAP
CTG-0160	NSCLC	Squamous cell carcinoma	Primary	Lung	I	64	Female	9	Carboplatin	98	Low
CTG-0160	NSCLC	Squamous cell carcinoma	Primary	Lung	I	64	Female	9	Carboplatin	90	Low
CTG-0163	NSCLC	Squamous cell carcinoma	Primary	Lung	III	52	Female	15	Carboplatin	72	Low
CTG-0163	NSCLC	Squamous cell carcinoma	Primary	Lung	III	52	Female	15	Carboplatin	76	Low
CTG-0743	NSCLC	Adenocarcinoma	Metastatic	Bone	IV	58	Male	8	Carboplatin	74	High
CTG-0743	NSCLC	Adenocarcinoma	Metastatic	Bone	IV	58	Male	8	Carboplatin	87	High
CTG-0781	Ovarian		Primary	Ovary	IV	67	Female		Carboplatin	96	Medium
CTG-0888	Breast	Invasive ductal carcinoma	Primary	Breast	III	43	Female	16	Carboplatin	104	High
CTG-0967	Mesothelioma	Epithelioid carcinoma	Primary	Pleura	II	61	Female	5	Carboplatin	-6	Low
CTG-0979	NSCLC	Adenocarcinoma	Primary	Lung	II	57	Female	25	Carboplatin	69	Low
CTG-0979	NSCLC	Adenocarcinoma	Primary	Lung	II	57	Female	25	Carboplatin	69	Low
CTG-0142	Sarcoma [Ewing sarcom	Small round blue cell carcinoma		Bone		17	Male		Cisplatin	100	Low
CTG-0143	Sarcoma [Ewing sarcom	Small round blue cell carcinoma		Bone marrow		22	Male		Cisplatin	100	Medium
CTG-0160	NSCLC	Squamous cell carcinoma	Primary	Lung	I	64	Female	9	Cisplatin	54	Low
CTG-0160	NSCLC	Squamous cell carcinoma	Primary	Lung	I	64	Female	9	Cisplatin	0	Low
CTG-0160	NSCLC	Squamous cell carcinoma	Primary	Lung	I	64	Female	9	Cisplatin	0	Low
CTG-0163	NSCLC	Squamous cell carcinoma	Primary	Lung	III	52	Female	15	Cisplatin	118	Low
CTG-0163	NSCLC	Squamous cell carcinoma	Primary	Lung	III	52	Female	15	Cisplatin	21	Low
CTG-0163	NSCLC	Squamous cell carcinoma	Primary	Lung	III	52	Female	15	Cisplatin	41	Low
CTG-0743	NSCLC	Adenocarcinoma	Metastatic	Bone	IV	58	Male	8	Cisplatin	100	High
CTG-0826	Colorectal	Adenocarcinoma	Metastatic	Liver	III	38	Female	8	Cisplatin	92	Medium
CTG-0888	Breast	Invasive ductal carcinoma	Primary	Breast	III	43	Female	16	Cisplatin	104	High
CTG-0941	Cholangiocarcinoma	Squamous cell carcinoma	Metastatic	Liver	IV	57	Female	15	Cisplatin	84	High
CTG-0967	Mesothelioma	Epithelioid carcinoma	Primary	Pleura	II	61	Female	5	Cisplatin	63	Low
CTG-0979	NSCLC	Adenocarcinoma	Primary	Lung	II	57	Female	25	Cisplatin	94	Low
CTG-0011	Cholangiocarcinoma	Adenocarcinoma	Primary	Bile duct	III	74	Male	7	Gemcitabine	96	High
CTG-0018	Breast	Colloid carcinoma	Metastatic	Lymph node	IV	48	Female	13	Gemcitabine	42	Low
CTG-0137	Esophageal	Adenocarcinoma	Metastatic	Liver	IV	56	Male	6	Gemcitabine	71	Low
CTG-0142	Sarcoma [Ewing sarcom	Small round blue cell carcinoma		Bone		17	Male		Gemcitabine	77	Low
CTG-0143	Sarcoma [Ewing sarcom	Small round blue cell carcinoma		Bone marrow		22	Male		Gemcitabine	25	Medium
CTG-0160	NSCLC	Squamous cell carcinoma	Primary	Lung	I	64	Female	9	Gemcitabine	0	Low
CTG-0163	NSCLC	Squamous cell carcinoma	Primary	Lung	III	52	Female	15	Gemcitabine	21	Low
CTG-0493	Esophageal	Adenocarcinoma	Metastatic	Liver			Male		Gemcitabine	55	Low
CTG-0676	Esophageal	Adenocarcinoma	Metastatic	Liver	IV	51	Female	11	Gemcitabine	100	Medium
CTG-0743	NSCLC	Adenocarcinoma	Metastatic	Bone	IV	58	Male	8	Gemcitabine	100	High
CTG-0781	Ovarian		Primary	Ovary	IV	67	Female		Gemcitabine	85	Medium
CTG-0791	Ovarian	Papillary serous adenocarcinon	Metastatic	Abdomen	III	48	Female	7	Gemcitabine	106	High
CTG-0798	Head and neck	Ductal adenocarcinoma	Metastatic	Lung	IV	37	Male	21	Gemcitabine	81	High

CTG-0826	Colorectal	Adenocarcinoma	Metastatic	Liver	III	38	Female	8	Gemcitabine	92	Medium
CTG-0835	Colorectal	Adenocarcinoma	Metastatic	Liver	IV	49	Female	15	Gemcitabine	40	Low
CTG-0888	Breast	Invasive ductal carcinoma	Primary	Breast	III	43	Female	16	Gemcitabine	104	High
CTG-0941	Cholangiocarcinoma	Squamous cell carcinoma	Metastatic	Liver	IV	57	Female	15	Gemcitabine	84	High
CTG-0967	Mesothelioma	Epithelioid carcinoma	Primary	Pleura	II	61	Female	5	Gemcitabine	63	Low
CTG-0979	NSCLC	Adenocarcinoma	Primary	Lung	II	57	Female	25	Gemcitabine	77	Low
CTG-0018	Breast	Colloid carcinoma	Metastatic	Lymph node	IV	48	Female	13	Paclitaxel	52	Low
CTG-0142	Sarcoma [Ewing sarcom	Small round blue cell carcinoma		Bone		17	Male		Paclitaxel	100	Low
CTG-0143	Sarcoma [Ewing sarcom	Small round blue cell carcinoma		Bone marrow		22	Male		Paclitaxel	0	Medium
CTG-0160	NSCLC	Squamous cell carcinoma	Primary	Lung	I	64	Female	9	Paclitaxel	58	Low
CTG-0160	NSCLC	Squamous cell carcinoma	Primary	Lung	I	64	Female	9	Paclitaxel	98	Low
CTG-0160	NSCLC	Squamous cell carcinoma	Primary	Lung	I	64	Female	9	Paclitaxel	90	Low
CTG-0160	NSCLC	Squamous cell carcinoma	Primary	Lung	I	64	Female	9	Paclitaxel	91	Low
CTG-0163	NSCLC	Squamous cell carcinoma	Primary	Lung	III	52	Female	15	Paclitaxel	69	Low
CTG-0163	NSCLC	Squamous cell carcinoma	Primary	Lung	III	52	Female	15	Paclitaxel	72	Low
CTG-0163	NSCLC	Squamous cell carcinoma	Primary	Lung	III	52	Female	15	Paclitaxel	76	Low
CTG-0163	NSCLC	Squamous cell carcinoma	Primary	Lung	III	52	Female	15	Paclitaxel	94	Low
CTG-0676	Esophageal	Adenocarcinoma	Metastatic	Liver	IV	51	Female	11	Paclitaxel	53	Medium
CTG-0743	NSCLC	Adenocarcinoma	Metastatic	Bone	IV	58	Male	8	Paclitaxel	74	High
CTG-0781	Ovarian		Primary	Ovary	IV	67	Female		Paclitaxel	96	Medium
CTG-0967	Mesothelioma	Epithelioid carcinoma	Primary	Pleura	II	61	Female	5	Paclitaxel	-6	Low
CTG-0979	NSCLC	Adenocarcinoma	Primary	Lung	II	57	Female	25	Paclitaxel	69	Low
CTG-0137	Esophageal	Adenocarcinoma	Metastatic	Liver	IV	56	Male	6	Sunitinib	91	Low
CTG-0137	Esophageal	Adenocarcinoma	Metastatic	Liver	IV	56	Male	6	Sunitinib	85	Low
CTG-0493	Esophageal	Adenocarcinoma	Metastatic	Liver			Male		Sunitinib	0	Low
CTG-0493	Esophageal	Adenocarcinoma	Metastatic	Liver			Male		Sunitinib	59	Low
CTG-0493	Esophageal	Adenocarcinoma	Metastatic	Liver			Male		Sunitinib	55	Low
CTG-0676	Esophageal	Adenocarcinoma	Metastatic	Liver	IV	51	Female	11	Sunitinib	100	Medium
CTG-0791	Ovarian	Papillary serous adenocarcinon	Metastatic	Abdomen	III	48	Female	7	Sunitinib	34	High
CTG-0826	Colorectal	Adenocarcinoma	Metastatic	Liver	III	38	Female	8	Sunitinib	83	Medium
CTG-0941	Cholangiocarcinoma	Squamous cell carcinoma	Metastatic	Liver	IV	57	Female	15	Sunitinib	97	High

Fig. S1

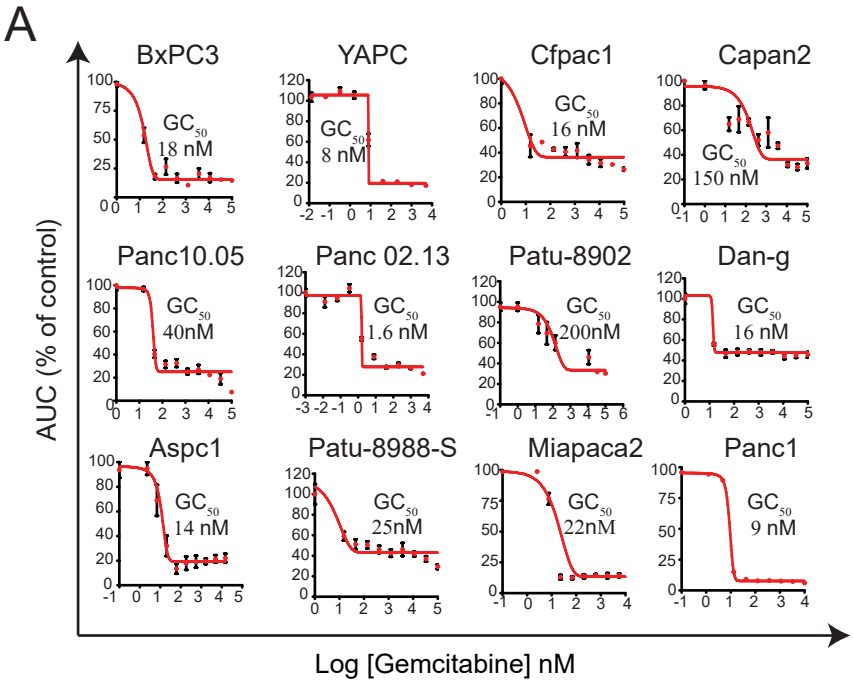
A
BxPC3
YAPC
Cfpac1
Capan2
Panc10.05
Panc 02.13
Patu-8902
Dan-g
Aspc1
Patu-8988-S
Miapaca2
Panc1
GC50 18 nM
GC50 8 nM
GC50 16 nM
GC50 150 nM
GC50 40nM
GC50 1.6 nM
GC50 200nM
GC50 16 nM
GC50 14 nM
GC50 25nM
GC50 22nM
GC50 9 nM
AUC (% of control)
Log [Gemcitabine] nM

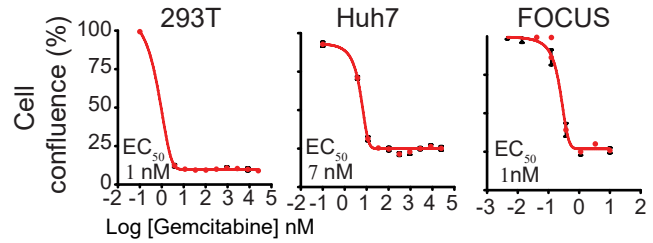
B
293T
Huh7
FOCUS
Cell confluence (%)
EC50 1 nM
EC50 7 nM
EC50 1nM
Log [Gemcitabine] nM

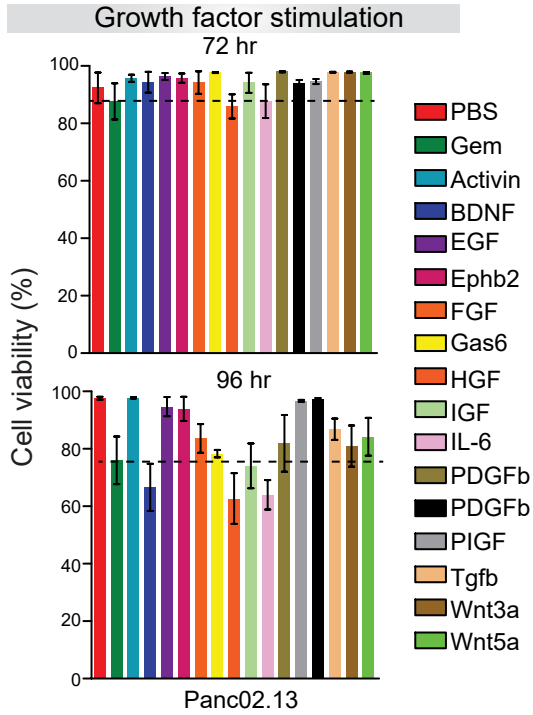
C
Growth factor stimulation
72 hr
96 hr
Cell viability (%)
Panc02.13
PBS
Gem
Activin
BDNF
EGF
Ephb2
FGF
Gas6
HGF
IGF
IL-6
PDGFb
PDGFb
PIGF
Tgfb
Wnt3a
Wnt5a

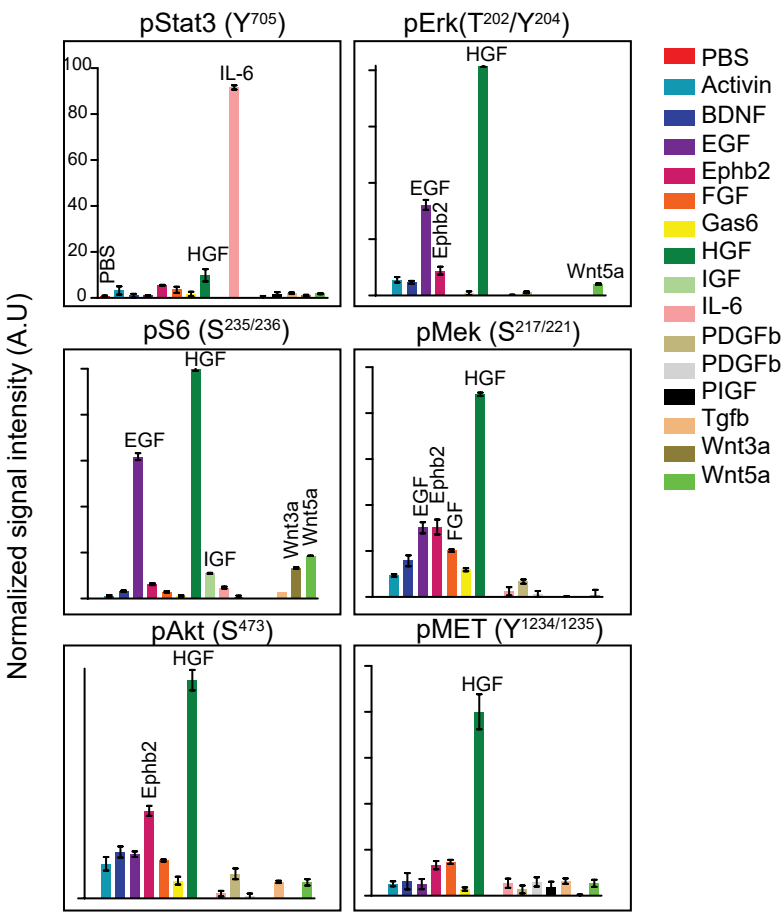
D
pStat3 (Y705)
pErk(T202/Y204)
pS6 (S235/236)
pMek (S217/221)
pAkt (S473)
pMET (Y1234/1235)
Normalized signal intensity (A.U)
PBS
Activin
BDNF
EGF
Ephb2
FGF
Gas6
HGF
IGF
IL-6
PDGFb
PDGFb
PIGF
Tgfb
Wnt3a
Wnt5a

Fig. S2

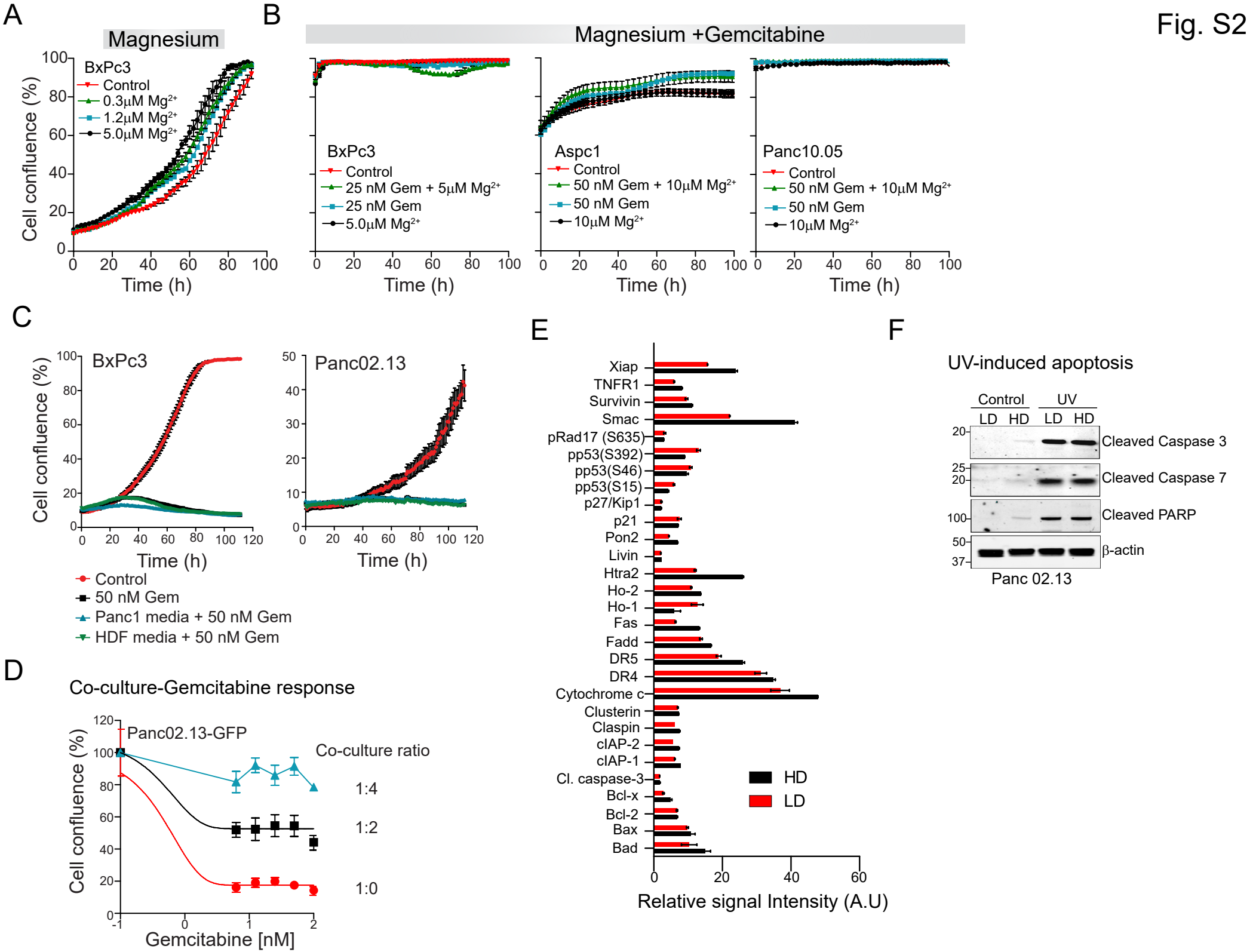
A
Magnesium
BxPc3
Control
0.3μM Mg2+
1.2μM Mg2+
5.0μM Mg2+
Cell confluence (%)
Time (h)
B
Magnesium +Gemcitabine
BxPc3
Control
25 nM Gem + 5μM Mg2+
25 nM Gem
5.0μM Mg2+
Aspc1
Control
50 nM Gem + 10μM Mg2+
50 nM Gem
10μM Mg2+
Panc10.05
Control
50 nM Gem + 10μM Mg2+
50 nM Gem
10μM Mg2+
C
BxPc3
Panc02.13
Control
50 nM Gem
Panc1 media + 50 nM Gem
HDF media + 50 nM Gem
D
Co-culture-Gemcitabine response
Panc02.13-GFP
Co-culture ratio
1:4
1:2
1:0
Gemcitabine [nM]
E
Xiap
TNFR1
Survivin
Smac
pRad17 (S635)
pp53(S392)
pp53(S46)
pp53(S15)
p27/Kip1
p21
Pon2
Livin
Htra2
Ho-2
Ho-1
Fas
Fadd
DR5
DR4
Cytochrome c
Clusterin
Claspin
cIAP-2
cIAP-1
Cl. caspase-3
Bcl-x
Bcl-2
Bax
Bad
HD
LD
Relative signal Intensity (A.U)
F
UV-induced apoptosis
Control
UV
LD
HD
LD
HD
Cleaved Caspase 3
Cleaved Caspase 7
Cleaved PARP
β-actin
Panc 02.13

Fig. S3

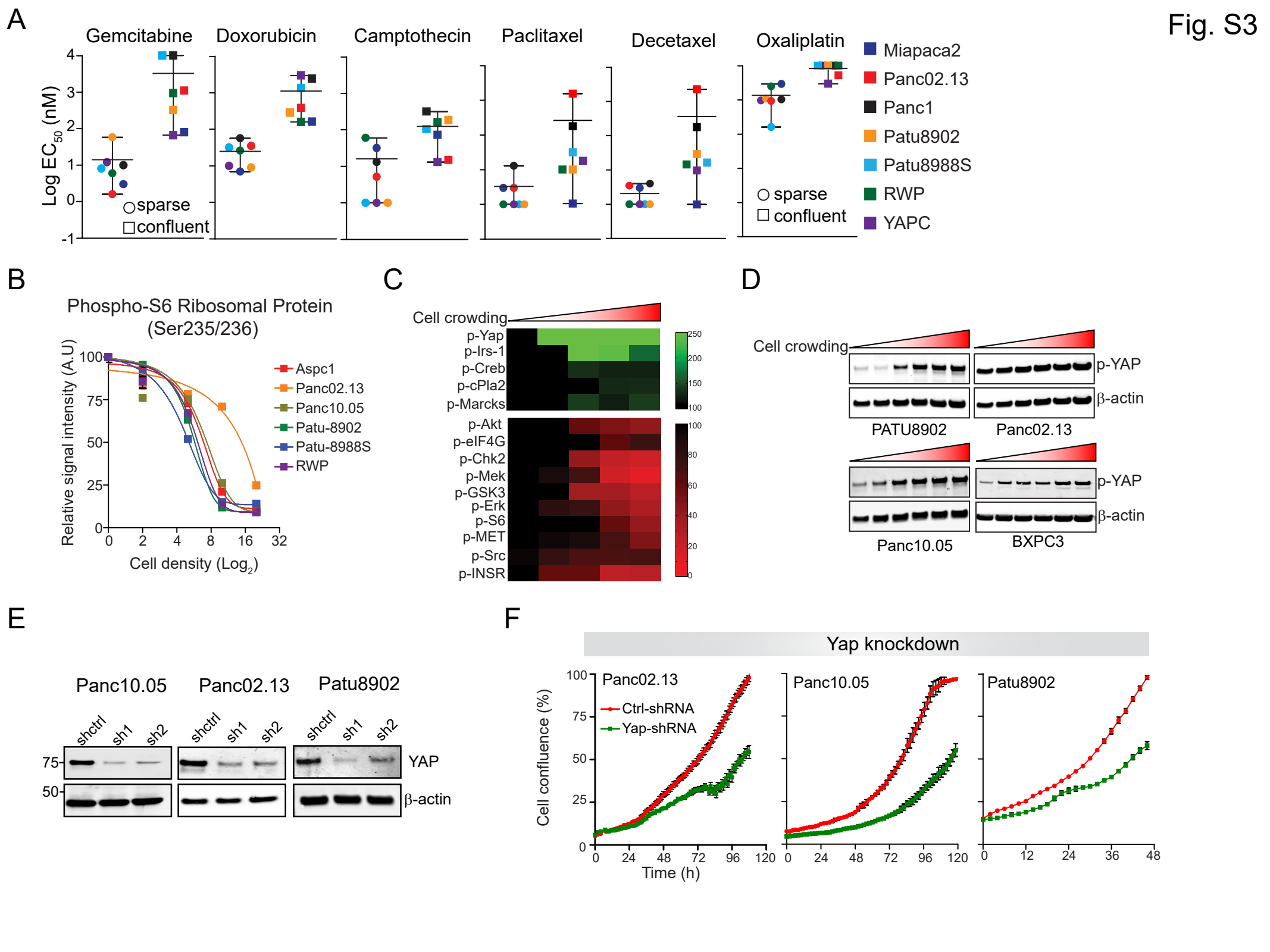
A
Gemcitabine
Doxorubicin
Camptothecin
Paclitaxel
Decetaxel
Oxaliplatin
Log EC50 (nM)
sparse
confluent
Miapaca2
Panc02.13
Panc1
Patu8902
Patu8988S
RWP
YAPC
B
Phospho-S6 Ribosomal Protein (Ser235/236)
Relative signal intensity (A.U)
Cell density (Log2)
Aspc1
Panc02.13
Panc10.05
Patu-8902
Patu-8988S
RWP
C
Cell crowding
p-Yap
p-Irs-1
p-Creb
p-cPla2
p-Marcks
p-Akt
p-eIF4G
p-Chk2
p-Mek
p-GSK3
p-Erk
p-S6
p-MET
p-Src
p-INSR
D
Cell crowding
p-YAP
β-actin
PATU8902
Panc02.13
Panc10.05
BXPC3
E
Panc10.05
Panc02.13
Patu8902
shctrl
sh1
sh2
YAP
β-actin
F
Yap knockdown
Panc02.13
Panc10.05
Patu8902
Ctrl-shRNA
Yap-shRNA
Cell confluence (%)
Time (h)

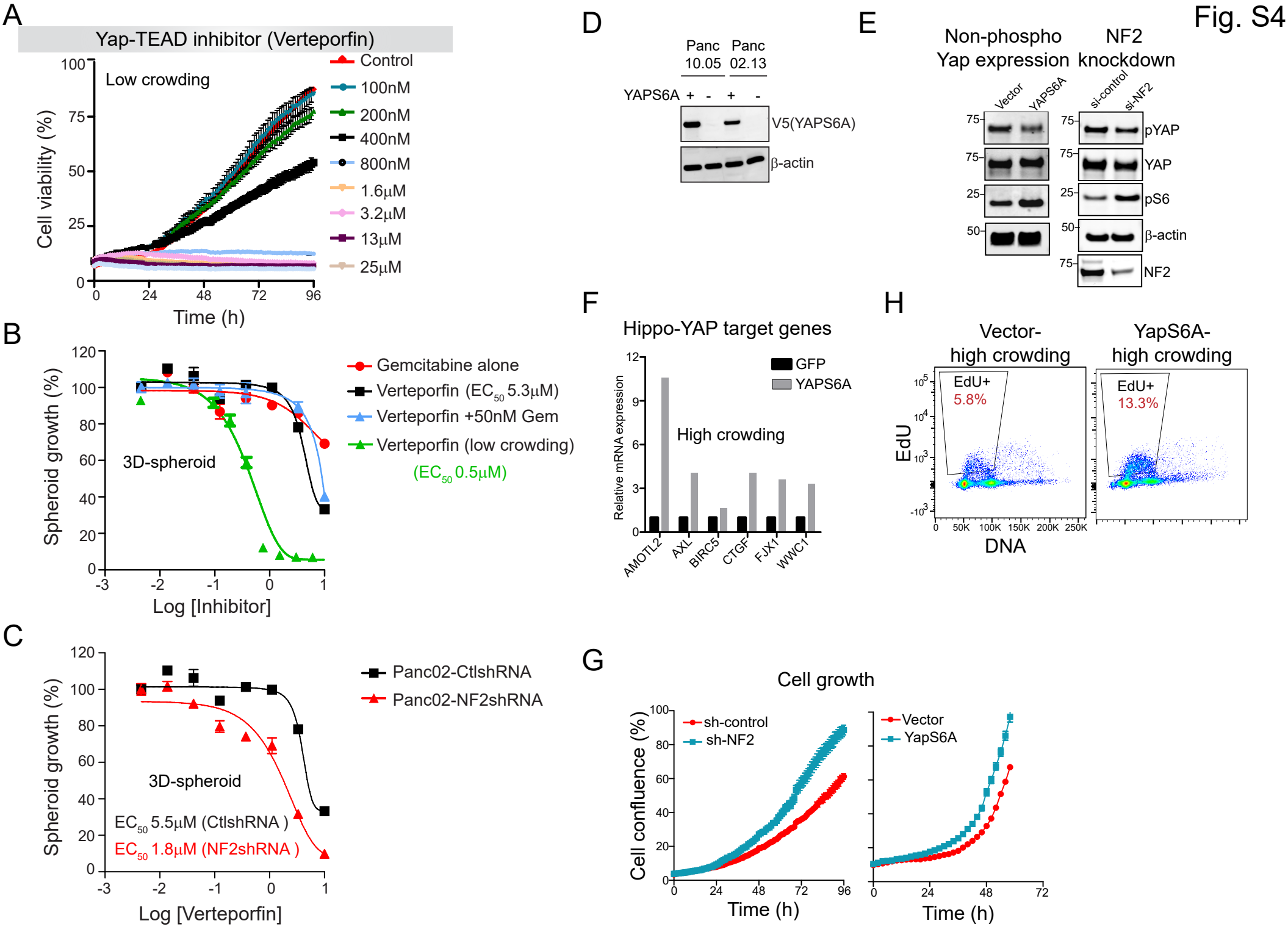
A
Yap-TEAD inhibitor (Verteporfin)
Low crowding
Cell viability (%)
Time (h)
Control
100nM
200nM
400nM
800nM
1.6μM
3.2μM
13μM
25μM
B
Spheroid growth (%)
3D-spheroid
Log [Inhibitor]
Gemcitabine alone
Verteporfin (EC50 5.3μM)
Verteporfin +50nM Gem
Verteporfin (low crowding)
(EC50 0.5μM)
C
Spheroid growth (%)
3D-spheroid
EC50 5.5μM (CtlshRNA)
EC50 1.8μM (NF2shRNA)
Log [Verteporfin]
Panc02-CtlshRNA
Panc02-NF2shRNA
D
Panc 10.05
Panc 02.13
YAPS6A + - + -
V5(YAPS6A)
β-actin
E
Non-phospho Yap expression
NF2 knockdown
Vector
YAPS6A
si-control
si-NF2
pYAP
YAP
pS6
β-actin
NF2
F
Hippo-YAP target genes
Relative mRNA expression
High crowding
GFP
YAPS6A
AMOTL2
AXL
BIRC5
CTGF
FJX1
WWC1
G
Cell growth
Cell confluence (%)
Time (h)
sh-control
sh-NF2
Vector
YapS6A
H
Vector-
high crowding
YapS6A-
high crowding
EdU+
5.8%
EdU+
13.3%
EdU
DNA

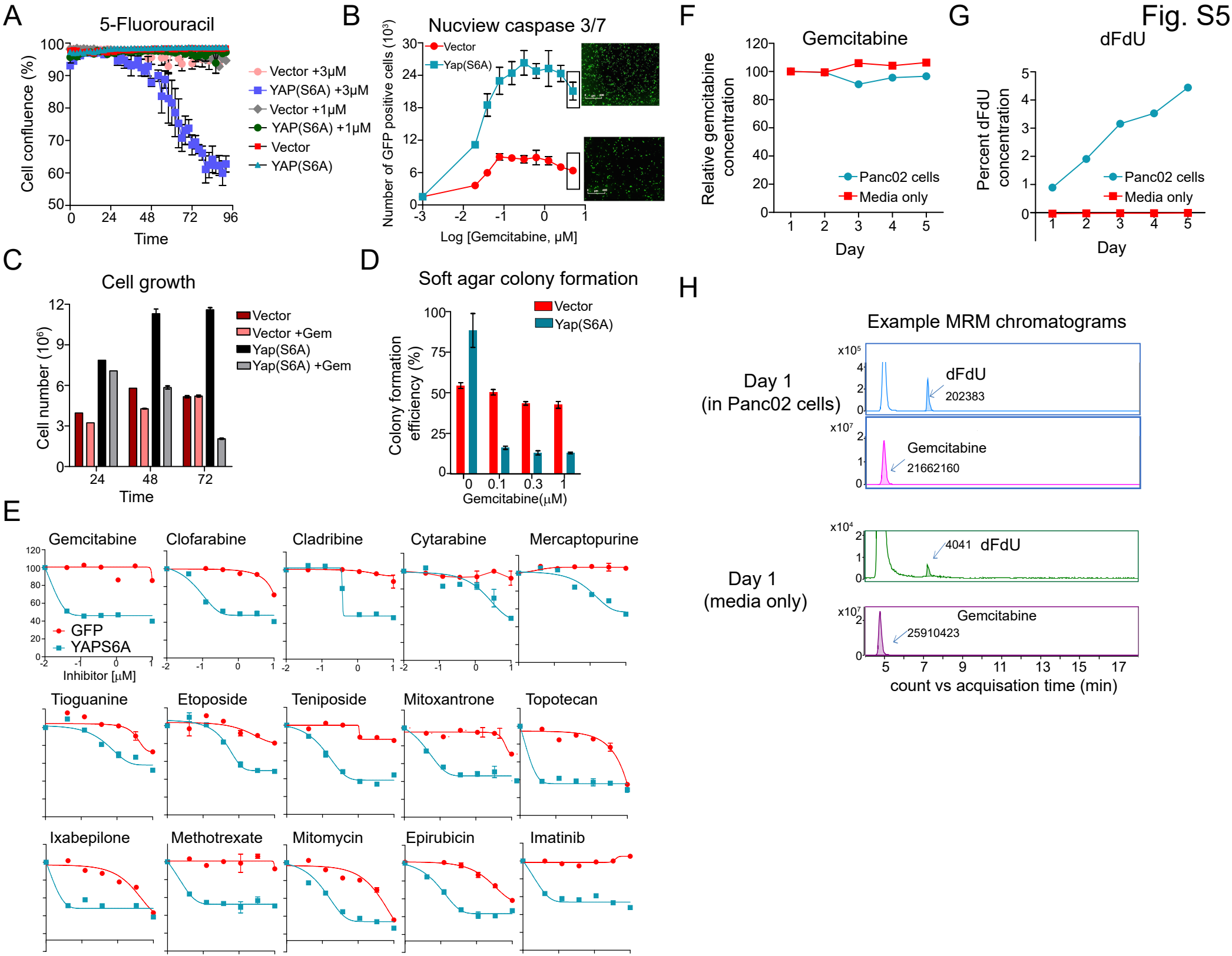
A
5-Fluorouracil
Cell confluence (%)
Time
Vector +3μM
YAP(S6A) +3μM
Vector +1μM
YAP(S6A) +1μM
Vector
YAP(S6A)
B
Nucview caspase 3/7
Number of GFP positive cells (10³)
Log [Gemcitabine, μM]
Vector
Yap(S6A)
C
Cell growth
Cell number (10⁶)
Time
Vector
Vector +Gem
Yap(S6A)
Yap(S6A) +Gem
D
Soft agar colony formation
Colony formation efficiency (%)
Gemcitabine(μM)
Vector
Yap(S6A)
E
Gemcitabine
Clofarabine
Cladribine
Cytarabine
Mercaptopurine
GFP
YAPS6A
Inhibitor [μM]
Tioguanine
Etoposide
Teniposide
Mitoxantrone
Topotecan
Ixabepilone
Methotrexate
Mitomycin
Epirubicin
Imatinib
F
Gemcitabine
Relative gemcitabine concentration
Day
Panc02 cells
Media only
G
dFdU
Percent dFdU concentration
Day
Panc02 cells
Media only
H
Example MRM chromatograms
Day 1
(in Panc02 cells)
dFdU
202383
Gemcitabine
21662160
Day 1
(media only)
4041 dFdU
Gemcitabine
25910423
count vs acquisation time (min)
Fig. S5

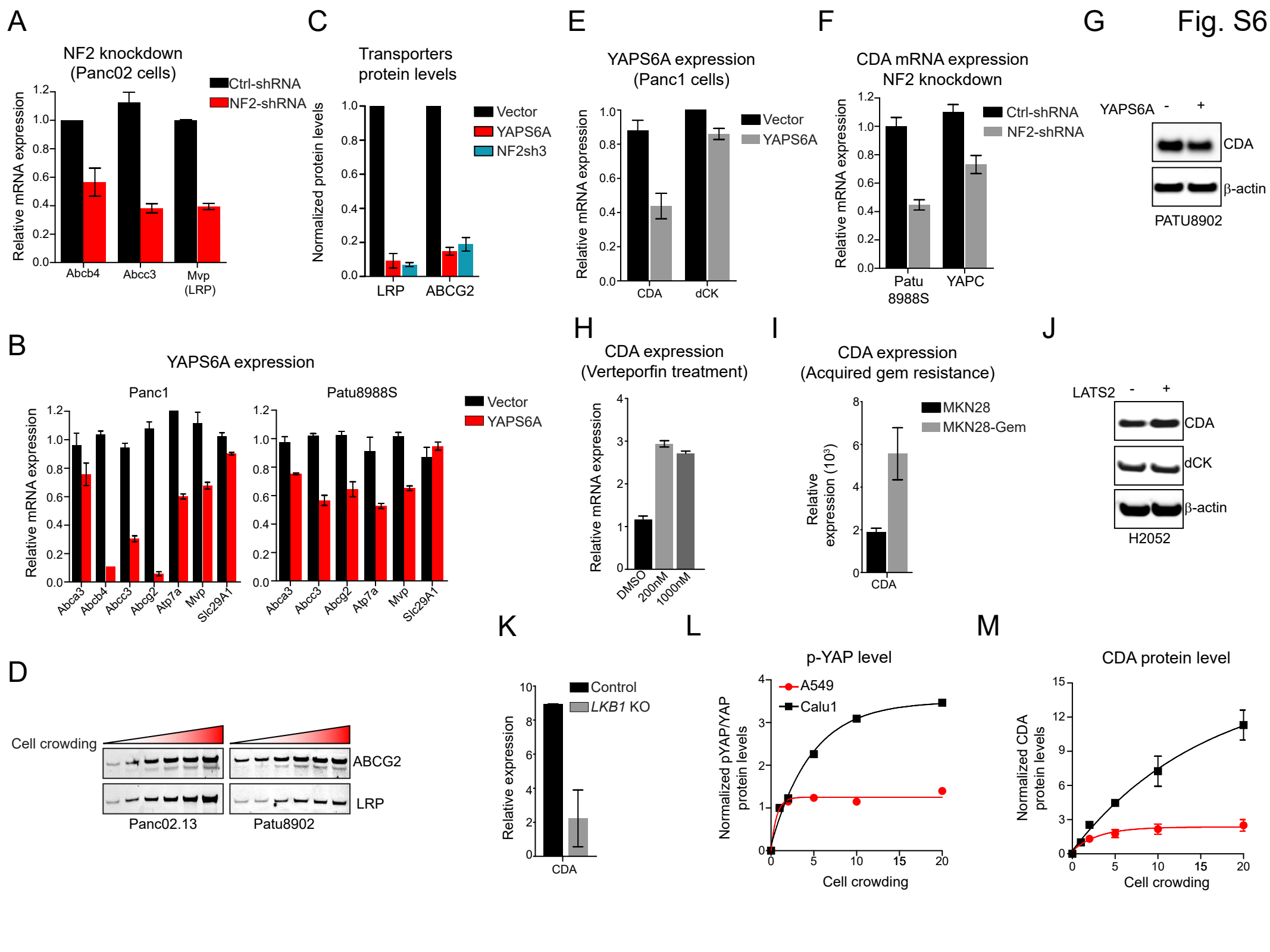
Fig. S6
A
NF2 knockdown
(Panc02 cells)
Ctrl-shRNA
NF2-shRNA
Relative mRNA expression
Abcb4
Abcc3
Mvp
(LRP)
B
YAPS6A expression
Panc1
Patu8988S
Vector
YAPS6A
Relative mRNA expression
Abca3
Abcb4
Abcc3
Abcg2
Atp7a
Mvp
Slc29A1
C
Transporters
protein levels
Vector
YAPS6A
NF2sh3
Normalized protein levels
LRP
ABCG2
D
Cell crowding
ABCG2
LRP
Panc02.13
Patu8902
E
YAPS6A expression
(Panc1 cells)
Vector
YAPS6A
Relative mRNA expression
CDA
dCK
F
CDA mRNA expression
NF2 knockdown
Ctrl-shRNA
NF2-shRNA
Relative mRNA expression
Patu
8988S
YAPC
G
YAPS6A - +
CDA
β-actin
PATU8902
H
CDA expression
(Verteporfin treatment)
Relative mRNA expression
DMSO
200nM
1000nM
I
CDA expression
(Acquired gem resistance)
MKN28
MKN28-Gem
Relative
expression (10³)
CDA
J
LATS2 - +
CDA
dCK
β-actin
H2052
K
Control
LKB1 KO
Relative expression
CDA
L
p-YAP level
A549
Calu1
Normalized pYAP/YAP
protein levels
Cell crowding
M
CDA protein level
Normalized CDA
protein levels
Cell crowding

Fig. S7

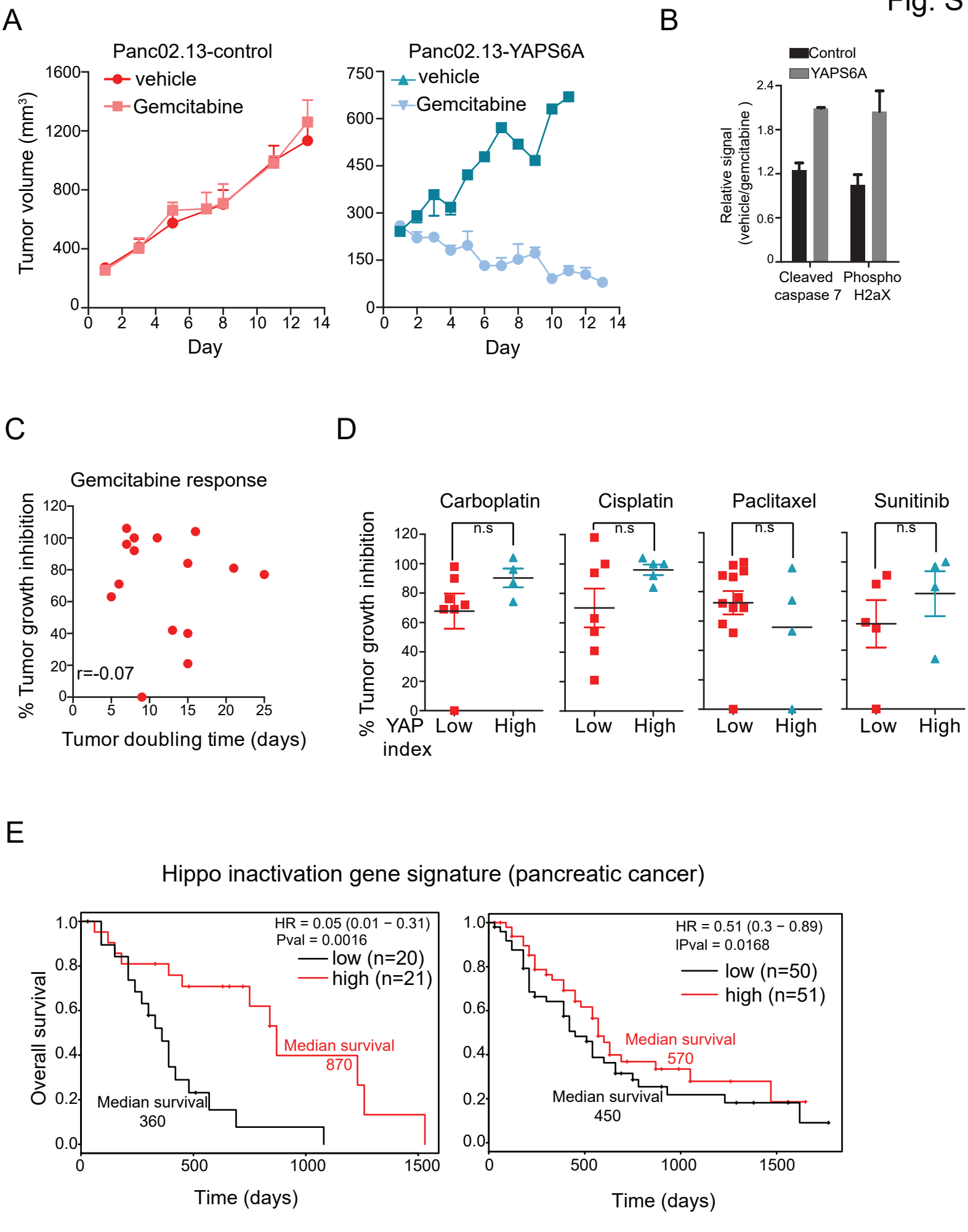
A
Panc02.13-control
vehicle
Gemcitabine
Tumor volume (mm3)
Day
Panc02.13-YAPS6A
vehicle
Gemcitabine
Day
B
Control
YAPS6A
Relative signal (vehicle/gemcitabine)
Cleaved caspase 7
Phospho H2aX
C
Gemcitabine response
% Tumor growth inhibition
r=-0.07
Tumor doubling time (days)
D
Carboplatin
Cisplatin
Paclitaxel
Sunitinib
% Tumor growth inhibition
n.s
YAP index
Low
High
E
Hippo inactivation gene signature (pancreatic cancer)
Overall survival
HR = 0.05 (0.01 − 0.31)
Pval = 0.0016
low (n=20)
high (n=21)
Median survival 870
Median survival 360
Time (days)
HR = 0.51 (0.3 − 0.89)
lPval = 0.0168
low (n=50)
high (n=51)
Median survival 570
Median survival 450
Time (days)

Fig. S8

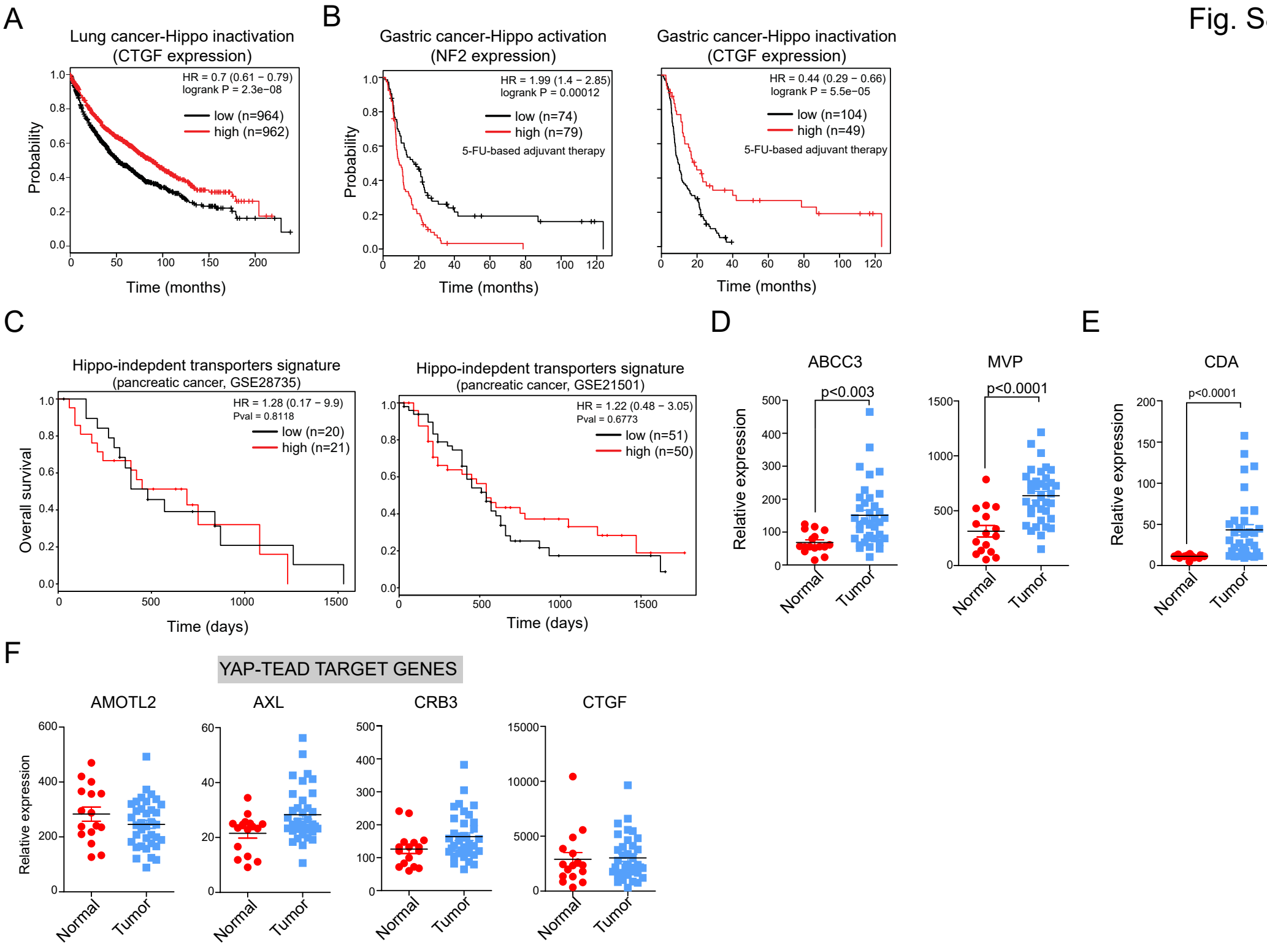
A
Lung cancer-Hippo inactivation
(CTGF expression)
HR = 0.7 (0.61 − 0.79)
logrank P = 2.3e−08
low (n=964)
high (n=962)
Probability
Time (months)
B
Gastric cancer-Hippo activation
(NF2 expression)
HR = 1.99 (1.4 − 2.85)
logrank P = 0.00012
low (n=74)
high (n=79)
5-FU-based adjuvant therapy
Probability
Time (months)
Gastric cancer-Hippo inactivation
(CTGF expression)
HR = 0.44 (0.29 − 0.66)
logrank P = 5.5e−05
low (n=104)
high (n=49)
5-FU-based adjuvant therapy
Time (months)
C
Hippo-indepdent transporters signature
(pancreatic cancer, GSE28735)
HR = 1.28 (0.17 − 9.9)
Pval = 0.8118
low (n=20)
high (n=21)
Overall survival
Time (days)
Hippo-indepdent transporters signature
(pancreatic cancer, GSE21501)
HR = 1.22 (0.48 − 3.05)
Pval = 0.6773
low (n=51)
high (n=50)
Time (days)
D
ABCC3
p<0.003
MVP
p<0.0001
Relative expression
Normal
Tumor
E
CDA
p<0.0001
Relative expression
Normal
Tumor
F
YAP-TEAD TARGET GENES
AMOTL2
AXL
CRB3
CTGF
Relative expression
Normal
Tumor